Gravitational waves from neutron star excitations in a binary inspiral

Alessandro Parisi[1,*] and Riccardo Sturani[2,†]

[1]ICTP-South American Institute for Fundamental Research, Instituto de Física Teórica (UNESP), 01140-070 São Paulo, Brazil

[2]International Institute of Physics (IIP), Universidade Federal do Rio Grande do Norte (UFRN), C.P. 1613, 59078-970 Natal, Rio Grande do Norte, Brazil

(Received 6 November 2017; published 27 February 2018)

In the context of a binary inspiral of mixed neutron star–black hole systems, we investigate the excitation of the neutron star oscillation modes by the orbital motion. We study generic eccentric orbits and show that tidal interaction can excite the f-mode oscillations of the star by computing the amount of energy and angular momentum deposited into the star by the orbital motion tidal forces via closed form analytic expressions. We study the f-mode oscillations of cold neutron stars using recent microscopic nuclear equations of state, and we compute their imprint into the emitted gravitational waves.

DOI: 10.1103/PhysRevD.97.043015

I. INTRODUCTION

After the historical detections of gravitational waves (GWs) by binary black holes (BHs) [1] and the equally historical observation of a binary neutron star (NS) merger [2,3], it is expected that NSs in mixed binary BH-NS systems will be detected routinely in the GW channel by the next LIGO-Virgo observation runs, with the current upper limits given in Ref. [4]. Binary systems of NSs are qualitatively different emitters of GWs than BH ones: At first approximation, mixed NS-BH can be treated in general relativity on equal footing as binary BH systems; however, the presence of matter in the GW source may lead to new detectable astrophysical effects in the GW signal that are not expected to appear in the binary BH case like, e.g., NS tidal deformations leaving an imprint in the GW signal [5,6] and breaking of the NS giving origin to a gamma ray burst or a more general electromagnetic counterpart [7], to name only the most studied effects.

Beside their direct phenomenological relevance, these effects carry information on the highly uncertain equation of state of the NS, thus making GW detection an invaluable probe of the internal structure of NSs. In this work, we focus on a specific effect in GW signals: A NS can be tidally deformed by the orbital motion in generic elliptic orbits, hence setting oscillations of the NS normal modes. The orbit being elliptical can induce resonant oscillations at a frequency much higher than the frequency scale set by the inverse of the orbital period, since, in general, NS oscillations are much higher than the orbital frequency of inspiral binary systems.

Quantifying this phenomenon in light of the exciting prospect of a future GW detection has been the subject of extensive investigations in the literature in a number of different contexts. The theoretical setup for studying such tidally induced NS oscillations has been provided in Refs. [8,9]. In Ref. [10], it was originally proposed that tidal encounters between a NS and a main-sequence star might lead to the formation of x-ray binaries in globular clusters. In Ref. [11], the effects of the tidal resonances for a *circular* orbital motion have been studied, with the result that, if the companion of a NS is a BH of mass $\geq 6\ M_{\odot}$, the g-mode resonance is unimportant, while the f-mode resonance may affect the orbital evolution just before the merging. Reference [12] considered the energy absorbed by tidal excitations in an *eccentric* orbit (but not their imprint in the GW form). Reference [13] computed the effect on the emitted GW phase of a resonant mode excitation by the circular inspiral motion. Rotating NSs were considered by Ref. [14] (including g modes and r modes) when the spin axis is aligned or antialigned with the orbital angular momentum axis. Reference [15] solved for the tidal deformation dynamics of a NS in an external field of a massive object, and recently Ref. [16] presented a framework for the discussion of binary NSs and mixed NS-BH oscillation mode excitation and detection via the GWs observed by a future GW detector such as the Einstein Telescope or Cosmic Explorer. Numerical results on the GW emission of tidally excited NS oscillations in the last stages of a coalescence have been given in Ref. [17], and, in Ref. [18], the imprint of resonant tidal on the gravitational waveform has been computed within the effective one-body description of the two-body orbital motion. Finally, in Ref. [19], the tidal resonant effects are investigated in the context of the Hamiltonian formalism, finding quantitative

*alessandro26@live.it
†riccardo@iip.ufrn.br

estimates of the acceleration of the inspiral evolution due to a tidal term in the evolution equation of the binary system.

In the present paper, we consider a nonrotating NS with two different equations of states [20,21] with the goal of translating resonant excitations of various f modes for NSs inspiraling binary NS-BH systems that move in an elliptical orbit into a quantitative prediction for the emitted GW form well in the inspiral phase.

Numerical simulations show that most of the energy released in gravitational waves is indeed transferred into f modes, which are characterized by a wave function free of nodes along the radial direction. We do not study the possibilities of exciting the g modes, because these modes are related to the presence of density discontinuities in the outer envelopes of NSs (see [22,23]), density discontinuities in the inner core as a consequence of phase transitions at a high density (as studied in Ref. [24]), and/or thermal gradients as for a proto-NS (see, e.g., [25]). In this paper, we do not consider the possibility of having discontinuities of the density; moreover, we focus on barotropic equations of state where the pressure depends only on the energy density, implying that all g modes degenerate to zero frequency, and, hence, we focus on the excitations of f-modes. Our study is based on the following simplifying assumptions: (i) We neglect BH rotation, and, thus, we treat the BH as a point particle with mass $M_{\rm BH}$; (ii) the hydrodynamic stability of the NS is computed using the Oppenheimer-Volkoff equations, but we use Newtonian equations to calculate the oscillation modes (see Appendix A); (iii) the NS does not rotate and we neglect viscous effects.

By implementing the formalism presented in Refs. [8,9], we find new general analytic expressions for the energy and angular momentum deposited into NS oscillations during the elliptic orbital motion, allowing us to compute the mass quadrupole which is sourcing GW emission and eventually compare it with the orbital quadrupole.

The outline of this paper is as follows: In Sec. II, we present the setup of the physical system under consideration, and we provide new analytic expressions for the dynamics of tidally induced NS oscillations, which are the main result of this paper. In Sec. III, we analyze quantitatively their GW emission. Finally, conclusions for the future detectability of NS oscillations in the GW channel are drawn in Sec. IV. We set the speed of light $c = 1$ throughout this paper.

II. COUPLING OF NEUTRON STAR OSCILLATION MODES TO ORBITAL MOTION

In this section, we study the tidal excitation of NS oscillation modes in nonrotating stars in an elliptical orbit. Our analysis will be general, but the astrophysical case we have in mind is that of a binary NS-BH system. The idea to compute the energy deposited in stellar oscillations by the tidal gravitational field is first described by Refs. [8,9].

In this paper, we use Newtonian linearized equations to calculate the oscillation modes. The use of Newtonian equations is consistent with our Newtonian description of tidal interactions. For the f mode, general relativistic effects are expected to modify our results of oscillation frequencies by not more than $GM_*/(R_*c^2) \sim 20\%$ (see [26]), where M_* and R_* are the mass and radius, respectively, of the NS, while damping times deviate at most by 15% from the empirical relations given in Ref. [27], however, still compatible with the results obtained in the recent Ref. [28].

We also neglect the spin Ω_s of the NS. When $\Omega_s \neq 0$, the normal modes of the star get more complicated, especially when Ω_s becomes comparable to the mode frequencies [29]. For $\Omega_s \equiv 0$, the eigenmodes can be adequately approximated by those of a nonrotating spherical star; the basic equations that governing the oscillations of stars are discussed in more detail in Appendix A.

The NS oscillations are excited by tidal forces while the NS is bound in a binary system with a black hole in an eccentric orbit whose evolution is driven by gravitational radiation. The distance $\mathcal{D}$ between two objects in an elliptic orbit can be parametrized by [see, e.g., Eq. (4.54) of Ref. [30]]

$$\mathcal{D} = \frac{a(1-e^2)}{1+e\cos\psi}, \tag{1}$$

a being the semimajor axis and e the eccentricity (with $\psi = 0$ corresponding to the periastron), and the *true anomaly* ψ is related to the *eccentric anomaly* u and time t via [see, e.g., Eqs. (4.57) and (4.58) of Ref. [30]]

$$\begin{aligned} \beta \equiv u - e\sin u &= \omega_0 t, \\ \cos\psi &= \frac{\cos u - e}{1 - e\cos u}, \end{aligned} \tag{2}$$

T being the orbital period, $\omega_0 \equiv 2\pi/T$, with the following relationships holding among orbital parameters:

$$\dot{\psi} = \frac{[G_N M a(1-e^2)]^{1/2}}{\mathcal{D}^2} \tag{3}$$

(where M is the total mass of the binary system and G_N the Newton constant), and the standard definition of the relativistic orbital parameter

$$x \equiv (G_N M \omega_0)^{2/3} = \frac{G_N M}{a}, \tag{4}$$

the last equality holding only at the Newtonian level.

In order to study quantitatively the effect of the gravitational force inducing oscillations into the NS and following the procedure outlined in Ref. [9], it is useful to expand the Newtonian potential in spherical harmonics [see, e.g., Eq. (3.70) of Ref. [31]], centered at the star as per

$$\frac{1}{|\mathcal{D}-r|}=\sum_{\ell=0}^{\infty}\sum_{m=-\ell}^{\ell}\frac{4\pi}{2\ell+1}\frac{r^{\ell}}{\mathcal{D}^{\ell+1}}Y^{*}_{\ell m}(\theta,\phi)Y_{\ell m}(\pi/2,\psi), \tag{5}$$

r, θ, and ϕ being coordinates of the mass elements of the NS, $\ell, |m| \leq \ell$ are the spherical harmonic indices, and the orbital motion is assumed to be planar (no spin-induced precession). Using Eq. (5) for the elliptic orbit, it will be useful to expand $e^{im\psi}/\mathcal{D}^{\ell+1}$ for generic ℓ into a Fourier series of the type

$$\frac{e^{im\psi}}{\mathcal{D}^{\ell+1}}=\frac{1}{a^{\ell+1}}\sum_{j=0}^{\infty}\{c_j^{(\ell,m)}(e)\cos(j\beta)+is_j^{(\ell,m)}(e)\sin(j\beta)\}. \tag{6}$$

The detailed calculation of the Fourier coefficients $c_j^{(\ell,m)}(e)$ and $s_j^{(\ell,m)}(e)$ and their analytic expressions are presented in Appendix B.

In order to perform an analytic quantitative analysis, we borrow here the framework of Ref. [12], where NS oscillations are modeled as a series of damped harmonic oscillator displacements $x_n(t)$ driven by an external force, that we can take as purely monochromatic:

$$\ddot{x}_n(t)+2\frac{\dot{x_n}(t)}{\tau_n}+\omega_n^2x_n(t)=C_j\cos(\omega_j t)+S_j\sin(\omega_j t), \tag{7}$$

where τ_n is the damping time [32], ω_n is related to the stellar mode frequency ν_n by $\nu_n=(\omega_n^2-1/\tau_n^2)^{1/2}/(2\pi)$, $\omega_j \equiv j\omega_0$ is the jth harmonic of the main orbital angular frequency ω_0, and C_j, S_j is the exciting force amplitude. The time scale of ω_j variation, $\tau_{\rm GW}$, is set by the GW radiation and via the Einstein quadrupole formula

$$\begin{aligned}\tau_{\rm GW}=\left(\frac{\dot{\omega_0}}{\omega_0}\right)^{-1}&\simeq\frac{5}{96\eta}(G_NM)^{-5/3}\omega_0^{-8/3}g^{-1}(e)\\&\simeq 50\ \text{sec}\left(\frac{\eta}{0.2}\right)^{-1}\left(\frac{x}{0.02}\right)^{-5/2}\\&\quad\times\left(\frac{\omega_0}{100\ \text{Hz}}\right)^{-1}g^{-1}(e),\end{aligned} \tag{8}$$

with $\eta \equiv M_*(M-M_*)/M^2$ and $g(e)$ a dimensionless factor depending on eccentricity alone (see Sec. 4.1.3 of Ref. [30]):

$$g(e)=\frac{1}{(1-e^2)^{7/2}}\left(1+\frac{73}{24}e^2+\frac{37}{96}e^4\right).$$

When $\tau_{\rm GW} \gg 2\pi/\omega_n$, we can consider the forcing term as monochromatic and Eq. (7) admits the exact analytic solution

$$\begin{aligned}&[(\omega_j^2-\omega_n^2)^2+4\omega_j^2/\tau_n^2]x_n(t)\\&=(\omega_n^2-\omega_j^2)(C_j\cos(\omega_j t)+S_j\sin(\omega_j t))\\&\quad+2\omega_j/\tau_n(C_j\sin(\omega_j t)-S_j\cos(\omega_j t)),\end{aligned} \tag{9}$$

the solution $x_n^{(h)}$ to the homogeneous equation being

$$x_n^{(h)}\propto e^{-t/\tau_n}\cos[(\omega_n^2-1/\tau_n^2)^{1/2}t+\phi_0]. \tag{10}$$

Fixing the integration constants of the homogeneous solution to have vanishing excitations at the onset of the forcing term (deep in the early inspiral), one can find an energy per unit of mass $\mathcal{E}$ per unit of time:

$$\dot{\mathcal{E}}=\frac{(C_j^2+S_j^2)\omega_j^2/\tau_n}{(\omega_j^2-\omega_n^2)^2+4\omega_j^2/\tau_n^2}. \tag{11}$$

Equation (11) is valid when the forcing term can be considered constant for a time span larger than τ_n; however, the forcing term is coherent only over a time τ_c approximately given by the geometric mean of the instantaneous orbital period and the GW-triggered decay time $\tau_{\rm GW}$ [13]:

$$\begin{aligned}\tau_c&\equiv\sqrt{\tau_{\rm GW}2\pi/\omega_0}\\&\simeq 2\ \text{sec}\left(\frac{\eta}{0.2}\right)^{-1/2}\left(\frac{x}{0.02}\right)^{-5/4}\left(\frac{\omega_0}{100\ \text{Hz}}\right)^{-1}g^{-1/2}(e).\end{aligned} \tag{12}$$

In our case $\tau_{n=0}$ can vary in the range 10^{-1}, 10^0, and 10^2 sec for, respectively, $\ell=2$, 3, 4; see Tables I and II. Energy is mostly absorbed by the $\ell=2$ mode and also in the $\ell=3$ at resonance, where Eq. (11) holds also for $\tau_n > \tau_c$ by replacing τ_n in Eq. (11) with the minimum of τ_c, τ_n.

The NS oscillation vectors $\vec{\zeta}(t,\vec{r})$ satisfy an equation of the type (see [34])

$$\left(\rho\frac{d^2}{dt^2}+\mathcal{L}\right)\vec{\zeta}(t,\vec{r})=-\rho\vec{\nabla}U(\vec{r}), \tag{13}$$

where $\mathcal{L}$ is an operator characterizing the internal restoring force of the star. In order to apply this toy model of a damped harmonic oscillator to the tidally excited NS oscillation, we decompose the oscillation field $\vec{\zeta}(t,\vec{r})$ into normal modes with factorized time and space dependence:

$$\vec{\zeta}(t,\vec{r})=\sum_{n,\ell,m}q_{n\ell m}(t)\vec{\xi}_{n\ell m}(\vec{r}), \tag{14}$$

where we have added the spherical harmonics ℓ, m labels and the spatial mode eigenfunctions $\xi_{n\ell m}$ satisfy

$$(\mathcal{L}-\rho\omega_n^2)\vec{\xi}_{n\ell m}=0, \tag{15}$$

allowing the identification of ω_n with the stellar frequency of the eigenmode. The differential equations the oscillation

mode fields ξ satisfy are summarized in Appendix A, which are solved for two different equations of state and three values of the central density of the NS, with the resulting mass, radius, frequency, and damping times (the last two depending on ℓ) reported in Appendix C for $2 \le \ell \le 4$.

It is also useful to expand the eigenmodes into a radial (r) and a poloidal (h) component:

$$\vec{\xi}_{n\ell m}(\vec{r}) = (\xi^{(r)}_{n\ell}(r)\hat{e}_r + r\xi^{(h)}_{n\ell}(r)\vec{\nabla})Y_{\ell m}(\theta,\phi) \quad (16)$$

and impose the normalization condition [35]

$$\begin{aligned}&\int d^3x\rho(r)\vec{\xi}^*_{n\ell m}\cdot\vec{\xi}_{n'\ell'm'}\\ &= \int drr^2\rho(r)(\xi^{(r)}_{n\ell}\xi^{(r)}_{n'\ell'} + \ell(\ell+1)\xi^{(h)}_{n\ell}\xi^{(h)}_{n'\ell'})\delta_{\ell,\ell'}\delta_{m,m'}\\ &= \rho_0 R_*^5\delta_{n,n'}\delta_{\ell,\ell'}\delta_{m,m'}, \end{aligned} \quad (17)$$

where $\rho(r)$, ρ_0, and R_* are, respectively, the density, central density, and radius of the NS and we used

$$\begin{aligned}&\int d\Omega Y_{\ell m}(\theta,\phi)Y^*_{\ell'm'}(\theta,\phi) = \delta_{\ell,\ell'}\delta_{m,m'},\\ &\int d\Omega r^2\vec{\nabla}Y_{\ell m}(\theta,\phi)\cdot\vec{\nabla}Y^*_{\ell'm'}(\theta,\phi) = \ell(\ell+1)\delta_{\ell,\ell'}\delta_{m,m'},\\ &\int d\Omega\vec{r}\cdot\vec{\nabla}Y_{\ell m}(\theta,\phi)\vec{r}\cdot\vec{\nabla}Y^*_{\ell'm'}(\theta,\phi) = \delta_{\ell,\ell'}\delta_{m,m'}, \end{aligned} \quad (18)$$

and the integral of products of spherical harmonics with an unequal number of derivatives vanishes for any ℓ, m, ℓ', m'.

By multiplying both members of Eq. (13) by $\rho(r)\xi^*_{n\ell m}(\vec{r})$, substituting the expansion in Eq. (5), and integrating over the NS volume, the mode $q_{n\ell m}(t)$ is singled out, and it satisfies an equation of the type (7):

$$\begin{aligned}&\ddot{q}_{n\ell m}(t) + \frac{2}{\tau_{n\ell}}\dot{q}_{n\ell m}(t) + \omega_n^2 q_{n\ell m}(t)\\ &= \frac{G_N M_{\rm BH}}{a^3}\left(\frac{R_*}{a}\right)^{\ell-2}Q_{n\ell}W_{\ell m}\\ &\quad\times\sum_j(c_j^{(\ell+1,m)}(e)\cos(j\beta) + is_j^{(\ell+1,m)}(e)\sin(j\beta)), \end{aligned} \quad (19)$$

where

$$\begin{aligned}W_{\ell m} &\equiv \frac{4\pi}{2\ell+1}Y_{\ell m}(\pi/2,0),\\ Q_{n\ell} &\equiv \frac{1}{\rho_0 R_*^{\ell+3}}\int_0^{R_*}drr^2\rho(r)\ell r^{\ell-1}(\xi^{(r)}_{n\ell} + (\ell+1)\xi^{(h)}_{n\ell}), \end{aligned} \quad (20)$$

and $M_{\rm BH}$ is the black hole mass. Note that the rhs of Eq. (19) is complex, but given the symmetries of the c, s coefficients: $W_{\ell m} = (-1)^\ell W_{\ell -m}$ (and $W_{\ell m} = 0$ if ℓ, m have different parity), $c_j^{\ell,m} = c_j^{\ell,-m}$, $s_j^{\ell,m} = -s_j^{\ell,-m}$ the sum of $\sum_m q_{n\ell m}\times Y_{\ell m}$ returns a real quantity. The modes $q_{n\ell m}$ thus satisfy an equation of the type (7) with the coefficients C_j, S_j replaced by

$$(C_j, S_j) \to \frac{G_N M_{\rm BH}}{a^3}\left(\frac{R_*}{a}\right)^{\ell-2}Q_{n\ell}W_{\ell m}(c_j^{(\ell,m)}(e), s_j^{(\ell,m)}(e)). \quad (21)$$

These expressions will be needed in Sec. III to compute the time-varying quadrupole associated to these oscillations, the source of GWs.

The rate of energy (per unit of mass, per unit NS radius) absorbed by each oscillation mode can be read from Eq. (11) by inserting the above values of C_j, S_j and summing over $n, j > 0, \ell \ge 2$ and $|m| \le \ell$, the rate of absorbed energy via tidal mechanism $\dot{E}_*$ being

$$\begin{aligned}\dot{E}_* &= \sum_j \dot{E}_j = \rho_0 R_*\left(\frac{R_*}{a}\right)^4\left(\frac{G_N M_{\rm BH}}{a}\right)^2\\ &\quad\times\sum_{j,n,\ell,m}(c_j^{(\ell,m)2} + s_j^{(\ell,m)2})\\ &\quad\times\left(\frac{R_*}{a}\right)^{2\ell-4}Q^2_{n\ell}W^2_{\ell m}\frac{\omega_j^2/\tau_{n\ell}}{(\omega_j^2-\omega^2_{n\ell})^2 + 4\omega_j^2/\tau^2_{n\ell}}. \end{aligned} \quad (22)$$

The contribution from individual j modes to the rate of energy absorption is plotted in Fig. 1 after being divided by the factor

$$\begin{aligned}K &\equiv \rho_0 R_*\left(\frac{R_*}{a}\right)^4\left(\frac{G_N M_{\rm BH}}{a}\right)^2\frac{(G_N M\omega_0)^2}{\omega_{02}}\\ &\simeq 1.5\times10^{-14}\ \frac{M_\odot}{\rm sec}\left(\frac{x}{0.01}\right)^9\left(\frac{\rho_0}{10^{15}\ {\rm gr/cm^3}}\right)\\ &\quad\times\left(\frac{R_*}{10\ {\rm Km}}\right)^5\left(\frac{M_{\rm BH}}{4\ M_\odot}\right)^2\left(\frac{M}{6\ M_\odot}\right)^{-6}, \end{aligned} \quad (23)$$

where $\omega_{02} = \omega_{n\ell}$ for $n = 0$, $\ell = 2$. Factorizing the absorbed energy rate by the quantity K has the virtue of making $\dot{E}_j/K$ dimensionless and independent of the relativistic parameter x (as long as the orbital frequency does not hit a resonance with $\omega_j \equiv j\omega_0$) and mildly dependent on ρ_0 and a.

In Fig. 2, we report the rate of absorbed energy $\dot{E}_*$ normalized by

$$\dot{E}_{\rm GW0} \equiv \frac{32}{5G_N}\eta^2 x^5, \quad (24)$$

which is the expression of the leading order in x of the GW emission rate at zero eccentricity from a binary inspiral, making visually easier the comparison between GW radiated energy $\dot{E}_{\rm GW}$ and $\dot{E}_*$. For $\dot{E}_{\rm GW}$ we use the 3PN formula taken from Ref. [37]; see also Sec. 10.3 of Ref. [38].

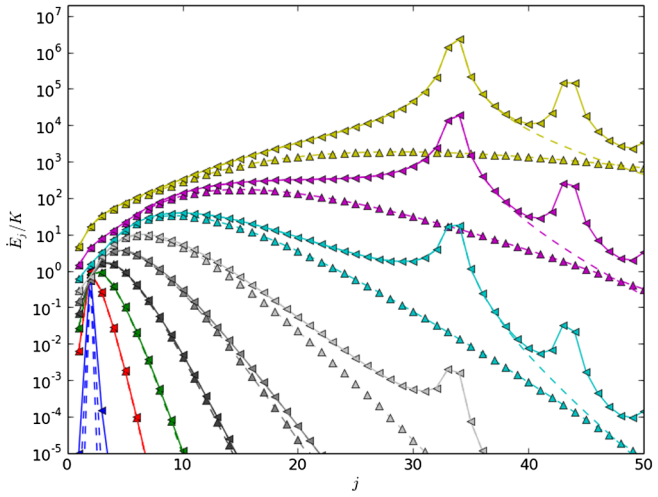

FIG. 1. Distribution of the rate of energy absorbed by the fundamental NS oscillation mode divided by K, defined in Eq. (23), as a function of the harmonic j of the fundamental mode in eccentric orbits, for nine equally spaced values of eccentricity (from $e_0 = 0$ in blue, through $e_i = i/10$ until $e_8 = 0.8$ in yellow). For each value of eccentricity, the curves for $x = 0.01$ and $x = 0.07$ are shown, with x defined in Eq. (4). For the latter value of x, the contribution of the $\ell = 2$ mode alone is isolated in the dashed curve. For $x = 0.07$, the resonant absorption peaks $\ell = 2$ are visible for $e = 0.5$, 0.6, 0.7, 0.8, and for $e = 0.6$, 0.7, 0.8 the resonant peak of $\ell = 3$ is also visible, as $\bar{j}\omega_0 = \bar{j}x^{3/2}/(G_N M) \simeq 18.1$ kHz$(\bar{j}/34)(6.965\ M_\odot/M)(x/0.07)^{3/2}$ where for this plot $M_{\rm BH} = 5\ M_\odot$ and we used the equation of state A (APR) of Ref. [20] and central density $\rho_0 = 1.5 \times 10^{15}$ gr/cm^3; see Table I. In this case, the $n = 0$ f mode has frequency $\nu_f^{\ell=2} = 2.888$ kHz [we have verified that for $x < 0.07$ the NS is safe from tidal breaking, whose condition requires $\mathcal{D} \lesssim 0.3 R_{\rm NS}(M_{\rm NS}/M_{\rm BH})^{1/3} x^{1/2}(M/M_{\rm BH})^{1/2}$; see [36]].

The absorbed angular momentum can be computed in a similar way, following Ref. [26], where it is noted that the variation of angular momentum

$$\dot{L}_* = -\int d^3x(\rho_0 + \delta\rho)(\hat{z}\cdot\vec{r}\times\vec{\nabla}U); \tag{25}$$

we can derive in our setup

$$\begin{aligned}\dot{L}_* &= \sum_{n\ell} q_{n\ell m}(t)\int d^3x\vec{\nabla}\cdot(\rho_0\vec{\xi}_{n\ell m})\frac{\partial U}{\partial\psi} \\ &= \sum_{n\ell m} q_{n\ell m}(t)\int d^3x\vec{\nabla}\cdot(\rho_0\vec{\xi}_{n\ell m})\frac{G_N M_{\rm BH}}{a}\left(\frac{r}{a}\right)^\ell W_{\ell m i m} \\ &\quad\times Y^*_{\ell m}(\theta,\phi)\sum_j (c_j^{(\ell,m)}(e)\cos(j\beta) + i s_j^{(\ell,m)}(e)\sin(j\beta)),\end{aligned} \tag{26}$$

where in the last passage we have inserted the expansion of Eqs. (5) and (6) and derived by parts inside the integral. In this form the angular momentum absorption rate by NS oscillations can be rewritten as

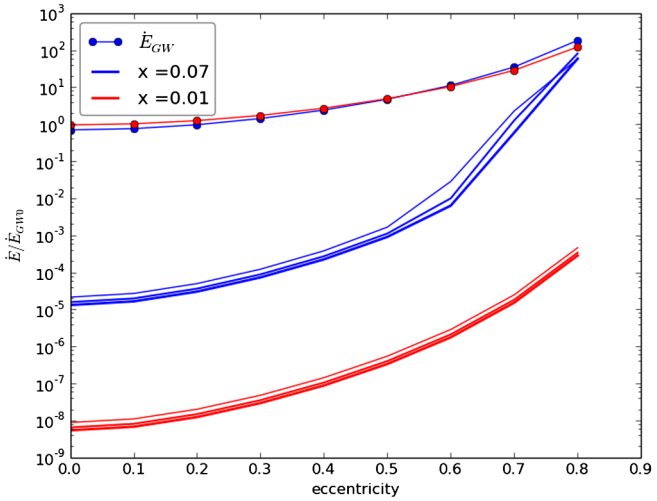

FIG. 2. Rate of energy absorbed $\dot{E}_*$ as a function of the eccentricity, with $M_{\rm BH} = 5\ M_\odot$, the NS with equation of state A (APR) of [20] for different values of the central density $\rho_0 = (1.5, 1.2, 0.99) \times 10^{15}$ gr/cm^3; lines of increasing thickness show results for increasing ρ_0. For comparison, we also plot the GW luminosity for the two values of x; all functions are divided by the Newtonian GW luminosity at zero eccentricity $\dot{E}_{\rm GW0}$ given by Eq. (24). Plots for the other equations of states described in Appendix C are shown in Fig. 7 and are qualitatively similar.

$$\dot{L}_* = \rho_0 R_*\left(\frac{G_N M_{\rm BH}}{a}\right)^2 2\sum_{j,n,\ell,m>0} m c_j^{(\ell,m)} s_j^{(\ell,m)}\left(\frac{R_*}{a}\right)^{2\ell} \times Q^2_{n\ell} W^2_{\ell m}\frac{\omega_j/\tau_{n\ell}}{(\omega_j^2 - \omega_{n\ell}^2)^2 + 4\omega_j^2/\tau_{n\ell}^2}. \tag{27}$$

In Fig. 3, the absorbed angular momentum rate $\dot{L}_*$ normalized by the leading-order expression in x of

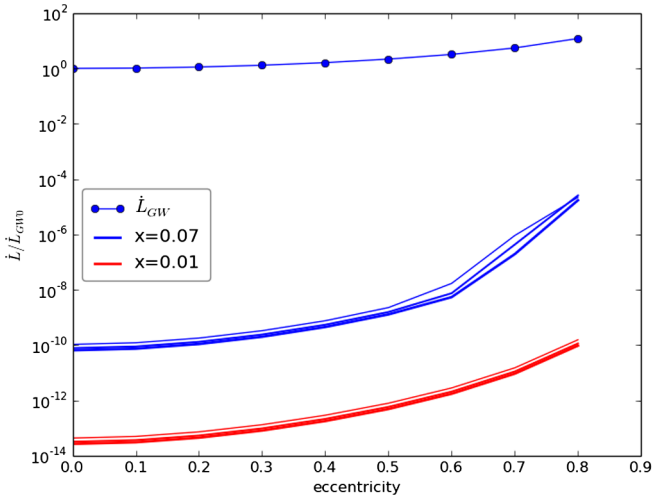

FIG. 3. Rate of angular momentum absorbed as a function of the eccentricity, the same parameters as in Fig. 2. Here $\dot{L}_{\rm GW}$ is the Newtonian angular momentum loss in GWs for small eccentricities $\dot{L}_{\rm GW} = \frac{32}{5}\eta^2 M\frac{x^{7/2}}{(1-e^2)^2}(1 + \frac{7}{8}e^2)$ and $\dot{L}_{\rm GW0} \equiv \dot{L}_{\rm GW}|_{e=0}$.

$\dot{L}_{\rm GW0} \equiv 32/5 M\eta^2 x^{7/2}$ is reported for various values of the relativistic parameter x and the eccentricity e. The values of $\dot{L}$ are negligible with respect to $\dot{L}_{\rm GW}$, and, given the typical moment of inertia of a NS ($\sim 10^{45}$ gr cm^2; see Ref. [39]), the induced rotation on the NS is also negligibly small.

III. GRAVITATIONAL WAVE EMISSION

We have seen in the previous section that the energy absorbed by the NS is very small compared to the orbital energy at moderate eccentricity values ($e \lesssim 0.6$); hence, such absorption will not alter in any significant way the chirping signal. However, the energy absorbed will set oscillations in the neutron star that give rise to a time-varying quadrupole, which will in turn generate GWs with a significantly different pattern than the GWs associated to the decaying orbital motion.

The general expression for the GW in the TT gauge is given by (see [40])

$$h_{ij}^{\rm TT}(t,r) = \frac{1}{r} G_N \sum_{\ell=2}^{+\infty} \sum_{m=-\ell}^{\ell} [u_{\ell m}(T^{E2}_{\ell m})_{ij} + v_{\ell m}(T^{B2}_{\ell m})_{ij}], \tag{28}$$

where $u_{\ell m}$ ($v_{\ell m}$) is linearly related to the ℓth time derivative of the mass (momentum) multipole moments. The leading-order contribution to the radiation reaction comes from the mass quadrupole term, for which it is (see, e.g., Sec. 3 of Ref. [30])

$$u_{2m} = \frac{16}{15}\pi\sqrt{3}\ddot{Q}^{ij}\mathcal{Y}^{2m*}_{ij}, \tag{29}$$

$\mathcal{Y}^{\ell m}_{i_1\ldots i_\ell}$ being the tensor spherical harmonics and $Q^{ij} \equiv \int d^3x \rho x^i x^j$ is the standard quadrupole mass moment in Cartesian coordinates. It will be convenient to express the leading-order GW amplitude in terms of the spherical components Q_m of the quadrupole, related to their Cartesian counterpart via

$$Q_{2m} \equiv \frac{8\pi}{15} Q_{ij}(\mathcal{Y}^{2m}_{ij})^*, \qquad Q_{ij} = \sum_{|m|\le 2} Q_{2m}\mathcal{Y}^{2m}_{ij}, \tag{30}$$

leading to (explicit expressions of $\ell = 2$ tensor spherical harmonics are reported in Appendix D)

$$u_{2m} = 2\sqrt{3}\ddot{Q}_m. \tag{31}$$

We now have all the ingredients to relate the leading GW source u_{2m} to the NS tidal oscillations via

$$Q_{*2m} = \frac{8\pi}{15}\int \rho r^2 Y^*_{2m} d^3x, \tag{32}$$

that in terms of the displacement vector introduced in Eqs. (13) and (14) can be expressed as (see [41])

$$\begin{aligned}\frac{15}{8\pi}Q_{*2m} &= \int (\rho_0 + \delta\rho) r^2 Y^*_{2m} d^3x \\ &= -\sum_n \int \vec{\nabla}\cdot(\rho_0 \vec{\xi}_{n2m}) r^2 Y^*_{2m} d^3x \\ &\simeq q_{02m}(t)\left(2\int_0^{R_*} \rho_0\{\xi^{(r)}_{02} + 3\xi^{(h)}_{02}\} r^3 dr \right. \\ &\quad \left. - \rho_0 \xi^{(r)}_{02} r^4|^{R_*}_0\right),\end{aligned} \tag{33}$$

where an integration by parts has been performed in the last step, the explicit expression of $\vec{\zeta}_{n2m}(t,\vec{x})$ has been inserted, and only the $n = 0$ contribution has been considered, since we analyzed only the f mode. Observing that the boundary term is numerically smaller than the integral term, substituting the solution of Eq. (19), and considering only the resonant contribution for $\omega_{\bar{j}} \simeq \omega_{02}$, the NS average quadrupole value can be written as

$$\begin{aligned}\langle Q^2_{*22}\rangle^{1/2} &\simeq \frac{2\sqrt{2}\pi}{15}\rho_0 R_*^5 Q^2_{02} W_{22}\frac{G_N M_{\rm BH}}{a^3}\frac{\tau_{02}}{\omega_{\bar{j}}} \\ &\quad \times [(c^{(2,2)}_{\bar{j}})^2 + (s^{(2,2)}_{\bar{j}})^2]^{1/2} \\ &\simeq \frac{4\sqrt{2}\pi}{15}\frac{(\rho_0 R_*^5 \tau_{02})^{1/2}}{\omega_{02}} Q_{02}\sqrt{\dot{E}^{(\ell=2)}_{\bar{j}}} \\ &\simeq 10^{-2}\, M_\odot\,{\rm km}^2\left(\frac{\rho_0}{10^{15}\,{\rm gr/cm^3}}\right)^{1/2}\left(\frac{R_*}{10\,{\rm km}}\right)^{5/2} \\ &\quad \times \left(\frac{\dot{E}^{(l=2)}_j}{10^{-8}\,M_\odot/{\rm sec}}\right)^{1/2}\left(\frac{\tau_{02}}{0.1\ {\rm sec}}\right)^{1/2}\left(\frac{\omega_{02}}{18\,{\rm kHz}}\right)^{-1}.\end{aligned} \tag{34}$$

The quantity directly related to GW emission, $u^{\rm (NS)}_{2m}$, follows straightforwardly via Eq. (31). In Fig. 4, we report the numerically derived contribution to the second time derivative of the quadrupole (divided by the reduced mass of the binary system) and, as a comparison, the (magnified) second derivative of the quadrupole associated to $n = 0$, $\ell = 2$ NS oscillations during an ordinary binary inspiral in which the orbit shrinks due to GW backreactions.

For comparison, we also report in Fig. 5 the time evolution of the displacement $q_{0\ell\ell}$ $\ell = 2$, 3, 4 along the inspiral phase.

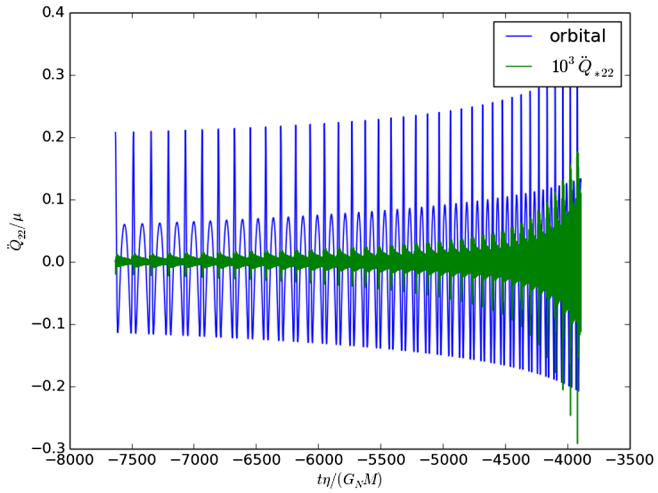

FIG. 4. Second derivative of the quadrupole $\ddot{Q}_{22}$ divided by the reduced mass $\mu \equiv \eta M$: the contribution from orbital dynamics compared with the (magnified) contribution from the NS oscillation Q_{*22} for an inspiral with initial conditions $x_i = 0.04$, $e_i = 0.4$, and $M_{\rm BH} = 5\ M_\odot$ and the parameter for the NS given by equation of state B (SLy4) [21] with $\rho_0 = 2 \times 10^{15}$ gr/cm^3.

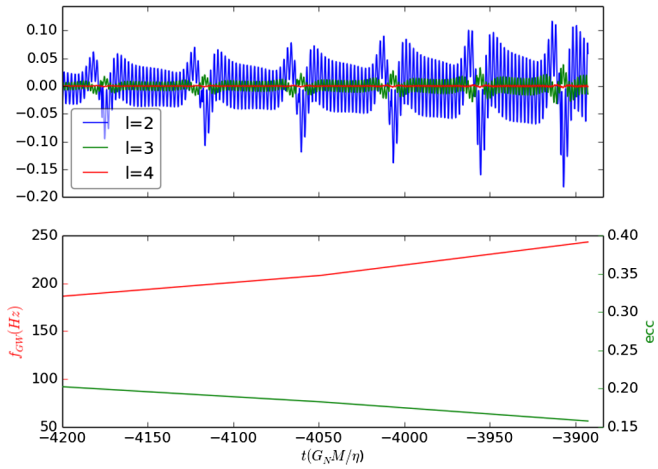

FIG. 5. Given the same parameters of Fig. 4, here are displayed the f-mode displacements $q_{0\ell\ell}$ for $\ell = 2, 3, 4$ (magnified by a factor of 10^3). Also shown are the main gravitational wave frequency $f_{\rm GW} \equiv \omega_0/\pi$ and the eccentricity along the inspiral dynamics considered.

IV. CONCLUSIONS

In this paper, we have developed and presented a framework able to perform analytic and quantitative study of the excitations of a neutron star in an inspiraling binary system of arbitrary eccentricity. We have computed the energy and the angular momentum deposited into stellar mode oscillations by the tidal field via closed form analytic formulas. The amount of energy absorbed by the neutron star in a given mode depends on the overlap of the tidal force field with the displacement field of the mode; hence, it requires solving the equilibrium equations of a neutron star, done here in the Newtonian approximation. We focused our analysis on the fundamental f mode of a nonrelativistic star, finding the rate of energy absorbed and angular momentum as a function of the eccentricity and of the period of the inspiral orbital, when the f mode can be in resonance with higher harmonics of the main orbital frequency and on their imprint in the gravitational wave signal well in the inspiral phase (note that this phenomenological effect is complementary to the acceleration of the coalescence because of the orbital energy leaking into tidal oscillations).

As a future development of this work, we intend to extend our analysis to the general relativistic equilibrium equations of a rotating neutron star, with the inclusion of the r mode and g modes, and considering a not barotropic equation of state: Such modes have lower frequency values than the f mode and can therefore be excited at resonance in an elliptical orbit earlier in the inspiral phase. The phenomenological impact of the computations presented here relies on the signature that neutron star oscillations will imprint onto the gravitational signals of an inspiral binary system. Despite being subdominant with respect to the gravitational wave sourced by the orbital motion, the detailed features of the star oscillation bears invaluable information on its equation of state and density, allowing us to make a bridge to the nuclear physics ruling its equilibrium. Since it is expected in the near future that a third-generation gravitational wave detector could observe signals from binary systems involving a neutron star at a signal-to-noise ratio of the order of 10^2 or more (see, e.g., [42]) and that such a detection will involve the observation of hundreds of thousands of gravitational wave cycles during the inspiral of a binary system for a time stretch of the order of several days, the quantitative prediction of the modification of the inspiral signal, even at a very low level, will have an impact on the physics outcome of the detection.

ACKNOWLEDGMENTS

The authors thank C. Chirenti for useful discussions. The work of A. P. has been supported by the FAPESP Grant No. 2016/00096-6, and R. S. has been supported by FAPESP Grant No. 2012/14132-3 during the early stage of this work.

APPENDIX A: FOUR FIRST-ORDER LINEAR DIFFERENTIAL EQUATIONS OF NONRADIAL OSCILLATIONS

The normal modes of a spherical star can be labeled by spherical harmonic indices ℓ and m and by a "radial quantum number" n. In spherical coordinates, the Lagrangian displacement ξ of a fluid element is given by

$$\xi_{n\ell m} = \left[\xi^{(r)}_{n\ell}(r), \xi^{(h)}_{n\ell}(r)\frac{\partial}{\partial\theta}, \frac{\xi^{(h)}_{n\ell}(r)}{\sin\theta}\frac{\partial}{\partial\phi}\right] Y_{\ell m}(\theta,\phi)e^{i\sigma t}, \tag{A1}$$

where $Y_{\ell m}$ denotes a spherical harmonic and σ denotes the pulsation angular frequency. The oscillation is assumed to be adiabatic; we ignore the thermal evolution of the NS, and for simplicity we use the Newtonian description in the Ref. [43] formulation. In this case, the equations reduce to a system of four first-order differential equations with four dimensionless variables, given by

$$y_1 = \frac{\xi^{(r)}_{n\ell}}{r}, \qquad y_2 = \frac{1}{gr}\left(\frac{p'}{\rho} + \Phi'\right) = \frac{\sigma^2}{g}\xi^{(h)}_{n\ell}, \tag{A2}$$

$$y_3 = \frac{\Phi'}{gr}, \qquad y_4 = \frac{1}{g}\frac{d\Phi'}{dr}. \tag{A3}$$

Here, the meanings of the symbols are as follows: p' and Φ' are the radial part of the Eulerian perturbation to the pressure p and the gravitational potential Φ, respectively; r is the distance from the center of the star, ρ is the density, and $g \equiv Gm(r)/r^2$ is the local acceleration due to gravity. The system of differential equations that governs the linear adiabatic oscillations of stars is then given by

$$r\frac{dy_1}{dr} = (V_g - 1 - \ell)y_1 + \left[\frac{\ell(\ell+1)}{c_1\omega^2} - V_g\right]y_2 + V_g y_3, \tag{A4}$$

$$r\frac{dy_2}{dr} = (c_1\omega^2 - A^*)y_1 + (3 - U + A^* - \ell)y_2 - A^* y_3, \tag{A5}$$

$$r\frac{dy_3}{dr} = (3 - U - \ell)y_3 + y_4, \tag{A6}$$

$$r\frac{dy_4}{dr} = A^* U y_1 + U V_g y_2 + [\ell(\ell+1) - U V_g]y_3 - (U + \ell - 2)y_4, \tag{A7}$$

where

$$V_g = -\frac{1}{\Gamma_1}\frac{d\ln p}{d\ln r} = \frac{gr}{c_s^2}, \qquad A^* = \frac{1}{\Gamma_1}\frac{d\ln p}{d\ln r} - \frac{d\ln\rho}{d\ln r}, \qquad U \equiv \frac{d\ln m(r)}{d\ln r} = \frac{4\pi\rho r^3}{m(r)}, \tag{A8}$$

$$c_1 \equiv \frac{r^3}{R_*^3}\frac{M_*}{m(r)}, \qquad \Gamma_1 = \left(\frac{\partial\ln p}{\partial\ln\rho}\right)_S, \qquad \omega^2 = \frac{R_*^3}{G_N M_*}\sigma^2. \tag{A9}$$

Here Γ_1 is the first adiabatic exponent, c_s is the sound speed, $m(r)$ is the concentric mass, M_* and R_* are the total mass and radius of the star, respectively, and G_N is the gravitational constant. There are four boundary conditions; the inner boundary conditions at $r = 0$ are

$$c_1\omega^2 y_1 - \ell y_2 = 0, \qquad \ell y_3 - y_4 = 0;$$

the outer boundary conditions at $r = R_*$ are

$$y_1 - y_2 + y_3 = 0, \qquad (\ell+1)y_3 + y_4 = 0.$$

The two central boundary conditions require that the two divergences involved, $\nabla\cdot\xi^{(r)}_{n\ell}$ and $\nabla\cdot\Phi'$, remain finite. At the surface, we require $\delta P/P$ to be finite and Φ', the gravitational force per unit mass, to be continuous across the perturbed surfaces. The above equations and boundary conditions constitute an eigenvalue problem for the eigenvalue σ.

The expression for the damping time due to the emission of gravitational waves in the Newtonian case (see [44,45]) is given by

$$\tau_{n\ell} \equiv \frac{(\ell-1)[(2\ell+1)!!]^2}{\ell(\ell+1)(\ell+2)}\left(\frac{\sigma}{2\pi G}\right)\left(\frac{c}{\sigma}\right)^{2\ell+1} \times \frac{\int_0^{R_*} dr\rho r^2[\xi^{(r)}_{n\ell}(r)^2 + \ell(\ell+1)\xi^{(h)}_{n\ell}(r)^2]}{\{\int_0^{R_*} dr\rho r^{\ell+1}[\xi^{(r)}_{n\ell}(r) + (\ell+1)\xi^{(h)}_{n\ell}(r)]\}^2}, \tag{A10}$$

where $n!! = 1\ldots(n-4)(n-2)n$.

APPENDIX B: EXPANSION OF THE FOURIER COEFFICIENTS

Expanding in Eq. (6), we have

$$c_j^{(\ell,m)}(e) = \frac{c_j}{\pi(1-e^2)^{\ell+1}}\int_{-\pi}^{\pi}\cos(m\psi)(1 + e\cos\psi)^{\ell+1} \times \cos(j\beta)d\beta, \tag{B1}$$

for $\ell \geq 0$, $|m| \leq l$, where we used that ψ is an odd function of time; hence $\cos\psi$ ($\sin\psi$) is an even (odd) function of time, $c_j = 1$ for $j \neq 0$, and $c_0 = 1/2$.

In order to expand $\cos(m\psi(t))$ into sums of terms of the type $\cos(n\beta)$, it is useful to express it in terms of powers of $\cos(\psi)$ via [46]

$$\cos(m\theta) = T_m(\cos(\theta)), \tag{B2}$$

where T_m is the Chebyshev polynomial of the order of r and it has the form

$$T_m(x) = \sum_{k=0}^{[m/2]} t_r^{(s)} x^{m-2k}, \tag{B3}$$

$[x]$ being the integer part of x. Using the standard relationships between eccentric anomaly ψ, true anomaly u, and time t (see Sec. II), one finds

$$1 + e\cos\psi = \frac{1-e^2}{1-e\cos u},$$
$$d\beta = (1 - e\cos u)du, \tag{B4}$$

to obtain

$$c_j^{(\ell,m)} = \frac{2c_n}{\pi}\int_0^\pi \sum_{k=0}^{[m/2]} t_m^{(k)} \frac{(\cos u - e)^{m-2k}}{(1-e\cos u)^{m-2k+\ell}} \times \cos(ju - je\sin u)du. \tag{B5}$$

In order to perform this integral, we use the standard Taylor expansions

$$(1-x)^n = \sum_{k=0}^{n}(-1)^k \frac{n!}{k!(n-k)!}x^k,$$
$$\frac{1}{(1-x)^n} = \sum_{k=0}^{\infty}\frac{(n+k-1)!}{k!(n-1)!}x^k \tag{B6}$$

to write

$$c_j^{(\ell,m)}(e) = \frac{2c_j}{\pi}\int_0^\pi \sum_{k=0}^{[m/2]} t_m^{(k)}(-e)^{m-2k}\sum_{p=0}^{m-2k}\frac{(m-2k)!}{p!(m-2k-p)!}(-1)^p\left(\frac{\cos u}{e}\right)^p \sum_{n=0}^{\infty}\frac{(m-2k+\ell+n-1)!}{n!(m-2k+\ell-1)!} \times (e\cos u)^n\cos(ju - je\sin u)du$$
$$= \frac{2c_j}{\pi}\int_0^\pi \sum_{k=0}^{[m/2]}\sum_{p=0}^{m-2k}\sum_{n=0}^{\infty}(-1)^{p+m}t_m^{(k)}\frac{(m-2k)!}{p!(m-2k-p)!}\frac{(m-2k+\ell+n-1)!}{n!(m-2k+\ell-1)!} \times e^{m-2k+n-p}(\cos u)^{p+n}\cos(ju - je\sin u)du, \tag{B7}$$

and then we use the de Moivre formula

$$\cos^n(u) = \frac{1}{2^n}\sum_{k=0}^{n}\frac{n!}{k!(n-k)!}\cos(n-2k)u \tag{B8}$$

to get to

$$c_j^{(\ell,m)}(e) = \frac{c_j}{\pi}\int_0^\pi \sum_{k=0}^{[m/2]}\sum_{p=0}^{m-2k}\sum_{n=0}^{\infty}\sum_{q=0}^{p+n}(-1)^{p+m}\frac{t_m^{(k)}}{2^{p+n-1}}\frac{(m-2k)!}{p!(m-2k-p)!}\frac{(m-2k+\ell+n-1)!}{n!(m-2k+\ell-1)!}\frac{(p+n)!}{q!(p+n-q)!} \times e^{m-2k+n-p}\cos[(p+n-2q)u]\cos(ju - je\sin u)du. \tag{B9}$$

Finally, using the integral representation of the Bessel functions

$$J_n(z) = \frac{1}{\pi}\int_0^\pi \cos(nu - z\sin u)du \tag{B10}$$

and the standard trigonometric identity

$$2\cos\alpha\cos\beta = \cos(\alpha+\beta) + \cos(\alpha-\beta), \tag{B11}$$

one gets to

$$c_j^{(\ell,m)}(e) = c_j(-e)^m \sum_{k=0}^{[m/2]} \sum_{p=0}^{m-2k} \sum_{n=0}^{\infty} \sum_{q=0}^{p+n} (-1)^p e^{n-2k-p} \frac{t_m^{(k)}}{2^{p+n}} \frac{(m-2k)!}{p!(m-2k-p)!} \frac{(m-2k+\ell+n-1)!}{n!(m-2k+\ell-1)!} \frac{(p+n)!}{q!(p+n-q)!} \times (J_{n+p+j-2q}(je) + J_{j-p-n+2q}(je)). \tag{B12}$$

Analogously for $s_j^{(\ell,m)}(e)$, one can use the Chebyshev polynomial of the second kind $U_n(x)$ satisfying the equation

$$\begin{aligned} \sin(m\theta) &= U_{m-1}(\cos\theta)\sin\theta \\ &= \sin\theta \sum_{k=0}^{[(m-1)/2]} u_{m-1}^{(k)} (\cos\theta)^{m-1-2k} \end{aligned} \tag{B13}$$

to obtain

$$\begin{aligned} s_j^{(\ell,m)}(e) &= \frac{2(1-e^2)^{1/2}}{\pi} \int_0^{\pi} \sin u \sum_{k=0}^{[(m-1)/2]} u_{m-1}^{(k)} \frac{(\cos u - e)^{m-1-2k}}{(1-e\cos u)^{m-2k+\ell}} \sin(ju - je\sin u) du \\ &= -\frac{2(1-e^2)^{1/2}}{\pi} \int_0^{\pi} \sum_{k=0}^{[(m-1)/2]} \sum_{p=0}^{m-1-2k} \sum_{n=0}^{\infty} \sum_{q=0}^{p+n} (-1)^{p+m} e^{m-1-2k+n-p} \frac{u_m^{(k)}}{2^{p+n}} \\ &\times \frac{(m-2k-1)!}{p!(m-2k-1-p)!} \frac{(m-2k+\ell+n-1)!}{n!(m-2k+\ell-1)!} \frac{(p+n)!}{q!(p+n-q)!} \sin u \cos[(p+n-2q)u] \sin(ju - je\sin u) du. \end{aligned} \tag{B14}$$

Now using

$$\begin{aligned} 2\sin\alpha\cos\beta &= \sin(\alpha+\beta) + \sin(\alpha-\beta), \\ 2\sin\alpha\sin\beta &= \cos(\alpha-\beta) - \cos(\alpha+\beta), \end{aligned} \tag{B15}$$

one finally obtains

$$s_j^{(\ell,m)}(e) = (1-e^2)^{1/2}(-e)^m \sum_{k=0}^{[(m-1)/2]} \sum_{p=0}^{m-1-2k} \sum_{n=0}^{\infty} \sum_{q=0}^{p+n} (-1)^p \frac{(m-2k-1)!}{p!(m-2k-1-p)!} \frac{(m-2k+\ell+n-1)!}{j!(m-2k+\ell-1)!} \frac{(p+n)!}{q!(p+n-q)!} \times e^{n-2k-p} \frac{u_{m-1}^{(k)}}{2^{p+n+1}} [J_{n+p+j+1-2q}(je) + J_{j-p-n+1+2q}(je) - J_{n+p+j-1-2q}(je) - J_{j-p-n-1+2q}(je)]. \tag{B16}$$

TABLE I. Data for the equation of state A (APR) [20] and [33] for the crust.

ρ_0 (gr/cm^3)	R (km)	M ($M_\odot$)	$\nu_{f,\ell=2}$ (kHz)	$\nu_{f,\ell=3}$ (kHz)	$\nu_{f,\ell=4}$ (kHz)	$\tau_{\ell=2}$ (s)	$\tau_{\ell=3}$ (s)	$\tau_{\ell=4}$ (s)	$\lvert Q_{02}\rvert$	$\lvert Q_{03}\rvert$	$\lvert Q_{04}\rvert$
1.5×10^{15}	11.132	1.965	2.888	3.742	4.420	0.153	4.494	67.1	2.321	2.437	2.613
1.2×10^{15}	11.433	1.704	2.741	3.456	4.033	0.158	3.28	181	2.258	2.482	2.501
9.9×10^{14}	11.603	1.408	2.384	3.071	3.602	0.204	2.939	152	2.323	2.594	2.653

TABLE II. Data for the equation of state B (SLy4) [21].

ρ_0 (gr/cm^3)	R (km)	M ($M_\odot$)	$\nu_{f,\ell=2}$ (kHz)	$\nu_{f,\ell=3}$ (kHz)	$\nu_{f,\ell=4}$ (kHz)	$\tau_{\ell=2}$ (s)	$\tau_{\ell=3}$ (s)	$\tau_{\ell=4}$ (s)	$\lvert Q_{02}\rvert$	$\lvert Q_{03}\rvert$	$\lvert Q_{04}\rvert$
2.0×10^{15}	10.615	1.994	3.300	4.143	4.829	0.152	4.48	60.2	2.148	2.372	2.443
1.6×10^{15}	11.017	1.884	3.024	3.808	4.461	0.149	3.17	196	2.180	2.439	2.446
1.2×10^{15}	11.435	1.634	2.654	3.372	3.967	0.168	8.53	130	2.270	2.989	2.508

APPENDIX C: NEUTRON STAR EQUATIONS OF STATE

This Appendix provides the numerical data for f-mode frequencies of two realistic equations of state. In the first part of the table of each equation of state, we list the central density, the radius, the mass of the stellar model, and the frequencies of the f mode for increasing values of ℓ. In the second part of each table, we list the damping times of NS and the coefficients $|Q_{0\ell}|$.

APPENDIX D: TENSOR SPHERICAL HARMONICS

The explicit expressions of the tensor spherical harmonics $\mathcal{Y}^{lm}_{i_1\ldots i_l}$ for $\ell = 2$ are

$$\mathcal{Y}^{22}_{ij} = \sqrt{\frac{15}{32\pi}}\begin{pmatrix} 1 & i & 0 \\ i & -1 & 0 \\ 0 & 0 & 0 \end{pmatrix}_{ij},$$

$$\mathcal{Y}^{21}_{ij} = -\sqrt{\frac{15}{32\pi}}\begin{pmatrix} 0 & 0 & 1 \\ 0 & 0 & i \\ 1 & i & 0 \end{pmatrix}_{ij},$$

$$\mathcal{Y}^{20}_{ij} = \sqrt{\frac{5}{16\pi}}\begin{pmatrix} -1 & 0 & 0 \\ 0 & -1 & 0 \\ 0 & 0 & 2 \end{pmatrix}_{ij}, \tag{D1}$$

and $\mathcal{Y}^{2,-m} = (-1)^m \mathcal{Y}^{2,m*}$.

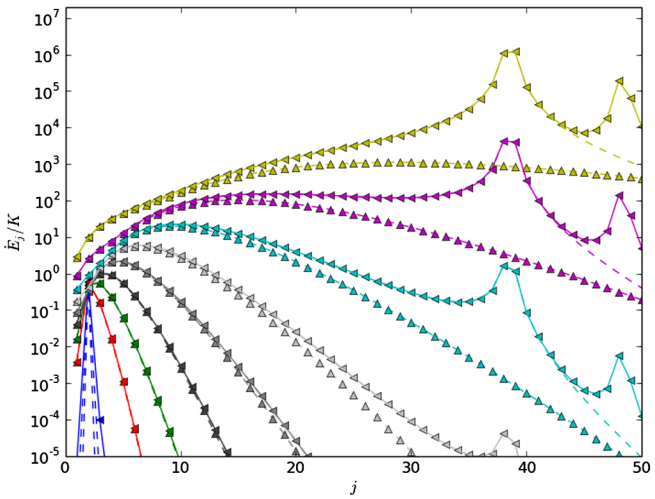

FIG. 6. Distribution of the energy per unit of mass absorbed by a single NS oscillation f mode $\dot{E}_j$ divided by the quantity K defined in Eq. (23) as a function of the harmonic mode j of the fundamental orbital frequency in eccentric orbits for the equation of state [21] in Table II for $\rho_0 = 2.0 \times 10^{15}$ gr/cm^3.

APPENDIX E: ENERGY AND ANGULAR MOMENTUM ABSORPTION RATES

In this Appendix, we report results for an additional equation of state than the one considered in the main text. Figure 6 shows the distribution of energy absorbed $\dot{E}_j$ as a

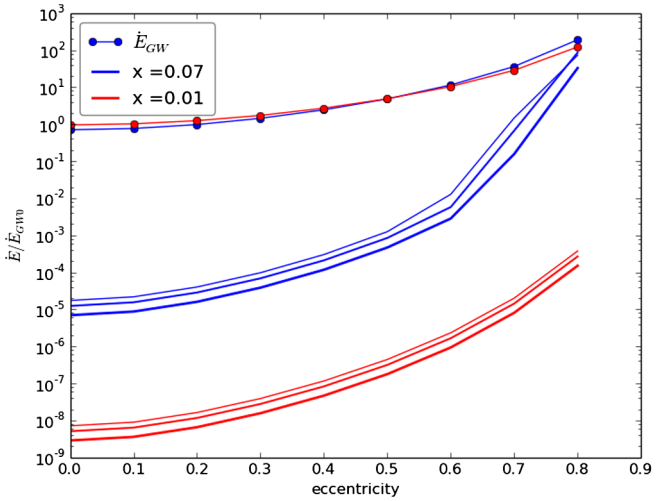

FIG. 7. Rate of energy absorbed $\dot{E}_*$ as a function of eccentricity, with $M_{\rm BH} = 5\ M_\odot$, NS with the equation of state given by Ref. [21] in Table II. For comparison, we also plot the GW luminosity for two values of x, and all functions are divided by the Newtonian GW luminosity at zero eccentricity $\dot{E}_{\rm GW0}$ given by Eq. (24). Note that for large eccentricity $e > 0.7$ absorption by the NS as computed in this approximation is not negligible compared to GW emission. For each equation of state, results for the three values of the central density reported in the corresponding tables are reported, with increasing line thickness denoting a higher central density.

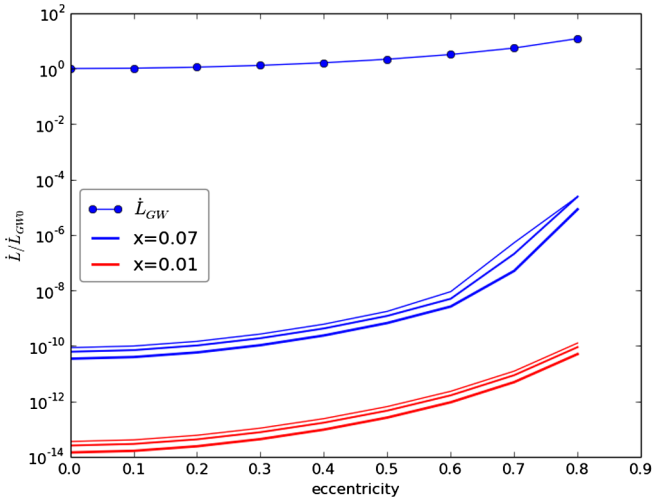

FIG. 8. Rate of angular momentum absorbed as a function of eccentricity, the same parameters as in Fig. 2. Here $\dot{L}_{\rm GW}$ is the Newtonian angular momentum loss in GWs for small eccentricities $\dot{L}_{\rm GW} = \frac{32}{5}\eta^2 M \frac{x^{7/2}}{(1-e^2)^2}(1+\frac{7}{8}e^2)$ and $\dot{L}_{\rm GW0} = \dot{L}_{\rm GW}|_{e=0}$, with $M \equiv M_* + M_{\rm BH}$, $\eta \equiv M_* M_{\rm BH}/M^2$.

function of the fundamental mode frequency harmonic j for the two equations of state in Tables I and II.

Figures 2 and 3 display, respectively, the energy and angular momentum absorbed by NS oscillations during the inspiral motion for three different central density for the equation of state reported in Table I. For comparison the gravitational luminosity and angular momentum emitted in gravitational wave are also reported. Analog quantities for the equation of state of Table II are reported in Figs 6–8.

[1] B. P. Abbott *et al.* (Virgo, LIGO Scientific Collaborations), Phys. Rev. X **6**, 041015 (2016).
[2] B. Abbott *et al.* (Virgo, LIGO Scientific Collaborations), Phys. Rev. Lett. **119**, 161101 (2017).
[3] B. P. Abbott *et al.* (GROND, SALT Group, OzGrav, DFN, INTEGRAL, Virgo, Insight-Hxmt, MAXI Team, Fermi-LAT, J-GEM, RATIR, IceCube, CAASTRO, LWA, ePESSTO, GRAWITA, RIMAS, SKA South Africa/MeerKAT, H. E. S. S., 1M2H Team, IKI-GW Follow-up, Fermi GBM, Pi of Sky, DWF (Deeper Wider Faster Program), Dark Energy Survey, MASTER, AstroSat Cadmium Zinc Telluride Imager Team, Swift, Pierre Auger, ASKAP, VINROUGE, JAGWAR, Chandra Team at McGill University, TTU-NRAO, GROWTH, AGILE Team, MWA, ATCA, AST3, TOROS, Pan-STARRS, NuSTAR, ATLAS Telescopes, BOOTES, CaltechNRAO, LIGO Scientific, High Time Resolution Universe Survey, Nordic Optical Telescope, Las Cumbres Observatory Group, TZAC Consortium, LOFAR, IPN, DLT40, Texas Tech University, HAWC, ANTARES, KU, Dark Energy Camera GW-EM, CALET, Euro VLBI Team, ALMA Collaborations), Astrophys. J. **848**, L12 (2017).
[4] B. P. Abbott *et al.* (Virgo, LIGO Scientific Collaborations), Astrophys. J. **832**, L21 (2016).
[5] L. Bildsten and C. Cutler, Astrophys. J. **400**, 175 (1992).
[6] É. É. Flanagan and T. Hinderer, Phys. Rev. D **77**, 021502 (2008).
[7] J. M. Lattimer and D. N. Schramm, Astrophys. J. **210**, 549 (1976).
[8] M. Turner, Astrophys. J. **216**, 914 (1977).
[9] W. Press and S. Teukolsky, Astrophys. J. **213**, 183 (1977).
[10] A. C. Fabian, J. E. Pringle, and M. J. Rees, Mon. Not. R. Astron. Soc. **172**, 15 (1975).
[11] M. Shibata, Prog. Theor. Phys. **91**, 871 (1994).
[12] Y. Rathore, R. D. Blandford, and A. E. Broderick, Mon. Not. R. Astron. Soc. **357**, 834 (2005).
[13] A. Reisenegger and P. Goldreich, Astrophys. J. **426**, 688 (1994).
[14] W. C. G. Ho and D. Lai, Mon. Not. R. Astron. Soc. **308**, 153 (1999).
[15] B. Carter and J.-P. Luminet, Astron. Astrophys. **121**, 97 (1983).
[16] C. Chirenti, R. Gold, and M. C. Miller, Astrophys. J. **837**, 67 (2017).
[17] R. Gold, S. Bernuzzi, M. Thierfelder, B. Brugmann, and F. Pretorius, Phys. Rev. D **86**, 121501 (2012).
[18] J. Steinhoff, T. Hinderer, A. Buonanno, and A. Taracchini, Phys. Rev. D **94**, 104028 (2016).
[19] K. D. Kokkotas and G. Schaefer, Mon. Not. R. Astron. Soc. **275**, 301 (1995).
[20] A. Akmal, V. R. Pandharipande, and D. G. Ravenhall, Phys. Rev. C **58**, 1804 (1998).
[21] F. Douchin and P. Haensel, Astron. Astrophys. **380**, 151 (2001).
[22] L. S. Finn, Mon. Not. R. Astron. Soc. **227**, 265 (1987).
[23] T. E. Strohmayer, Astrophys. J. **417**, 273 (1993).
[24] H. Sotani, K. Tominaga, and K.-I. Maeda, Phys. Rev. D **65**, 024010 (2001).
[25] V. Ferrari, G. Miniutti, and J. A. Pons, Mon. Not. R. Astron. Soc. **342**, 629 (2003).
[26] D. Lai, Mon. Not. R. Astron. Soc. **270**, 611 (1994).
[27] N. Andersson and K. D. Kokkotas, Mon. Not. R. Astron. Soc. **299**, 1059 (1998).
[28] G. Lioutas and N. Stergioulas, Gen. Relativ. Gravit. **50**, 12 (2018).
[29] E. Gaertig and K. D. Kokkotas, Phys. Rev. D **78**, 064063 (2008).
[30] M. Maggiore, *Gravitational Waves* (Oxford University, New York, 2008).
[31] D. Jackson, *Classical Electrodynamics* (Wiley, New York, 1998).
[32] As a possible mechanism for the damping of nonradial NS oscillations, we take the gravitational emission; we do not consider neutrino losses, radiative heat leakage, and magnetic damping.
[33] P. Haensel and J. L. Zdunik, Astron. Astrophys. **480**, 459 (2008).
[34] A. G. Kosovichev and I. D. Novikov, Mon. Not. R. Astron. Soc. **258**, 715 (1992).
[35] Note that with the normalization chosen $\xi^{(r,h)}_{n\ell}$ have a dimension of length and $q_{n\ell m}$ is dimensionless. However, the normalization can be arbitrarily chosen without affecting physical results, and our choice has the advantage of making following the formulas simpler.
[36] M. Vallisneri, Phys. Rev. Lett. **84**, 3519 (2000).
[37] K. G. Arun, L. Blanchet, B. R. Iyer, and M. S. S. Qusailah, Phys. Rev. D **77**, 064035 (2008).
[38] L. Blanchet, Living Rev. Relativity **17**, 2 (2014).
[39] P. Haensel, A. Y. Potekhin, and D. G. Yakovlev, *Neutron Stars 1: Equation of State and Structure* (Springer, New York, 2007).
[40] K. S. Thorne, Rev. Mod. Phys. **52**, 299 (1980).

[41] G. Ushomirsky, C. Cutler, and L. Bildsten, Mon. Not. R. Astron. Soc. **319**, 902 (2000).
[42] M. Punturo *et al.*, Classical Quantum Gravity **27**, 194002 (2010).
[43] W. A. Dziembowski, Acta Astronomica **21**, 289 (1971).
[44] K. S. Thorne, Astrophys. J. **158**, 997 (1969).
[45] E. Balbinski and B. F. Schutz, Mon. Not. R. Astron. Soc. **200**, 43P (1982).
[46] M. Abramowitz and I. Stegun, *Handbook of Mathematical Functions* (Dover, New York, 1964).